

Sensitivity of spatial photoelectron distributions to the absolute phase of an ultrashort intense laser pulse

Szczepan Chelkowski and André D. Bandrauk

Laboratoire de Chimie Théorique, Faculté des Sciences, Université de Sherbrooke, Sherbrooke, Québec, Canada J1K 2R1

(Received 24 January 2002; published 17 June 2002)

Using numerical solutions of the three-dimensional time-dependent Schrödinger equation (TDSE) for the hydrogen atom in an intense, ultrashort, i.e., few-cycle, linearly polarized laser pulse, we demonstrate that ionization yields measured in the forward direction ($0 < \theta < 15^\circ$) depend strongly (by a factor of 2) on the carrier phase, leading to considerable directional (forward or backward) photoelectron asymmetries along the laser polarization vector. This effect vanishes for pulses comprising more than 15 cycles. The phase dependence of photoelectron asymmetry is intensity-dependent: the strongest asymmetry is found in the intermediate multiphoton-tunneling regime, where asymmetry originates from the Coulomb attraction after tunneling. The character of asymmetry drastically changes when an electron ionizes in the barrier-suppression regime. A measurement method of the absolute phase and width, based on this directional effect, is proposed for linearly polarized ultrashort laser pulses.

DOI: 10.1103/PhysRevA.65.061802

PACS number(s): 42.65.Re, 32.80.Rm, 42.65.Ky, 42.50.Hz

During the past decade, considerable progress has been made in laser technology, allowing to shape and control intense laser pulses consisting only of a few optical cycles, i.e., a few femtoseconds [1]. The electric field envelope of such pulses varies significantly during one cycle, which may cause such pulses interacting with matter to induce physical phenomena depending on the absolute carrier phase, by which we mean the phase of carrier frequency with respect to the pulse envelope. For long pulses, the absolute phase of the pulse does not induce any measurable effect; in particular, the angular photoelectron distributions $f(\theta)$ are symmetric, i.e., $f(\theta) = f(\pi - \theta)$ (where θ is the angle between the photoelectron momentum and the laser polarization vector), because of the inversion symmetry of the monochromatic electric field and of the atom. Considerable variation of the field envelope during one cycle and the nonlinear response of the atom may lead to an asymmetry in space of the photoelectrons, thus this asymmetry may become a measurable signature of the absolute phase of the ultrashort laser pulse. Such spatial photoelectron asymmetries for long two-color ($\omega + 2\omega$) pulses, depending on the relative phase between the two colors, were extensively studied earlier [2–7]. In particular, in [6] the importance of the addition of the Coulomb potential in electron dynamics after tunneling was emphasized. So far, to our knowledge, such spatial (forward or backward) photoelectron asymmetries induced by the absolute phase of a single frequency but a few-cycle, linearly polarized laser pulse have not yet been investigated with the help of numerical solutions of the time-dependent Schrödinger equation (TDSE). It has been found that total ionization rates are very slightly (a few percent) dependent on the absolute phase [1,8]. Recent results based on numerical solution of the TDSE show the strong sensitivity of the harmonic spectra to the absolute phase of the laser [10]. We show in the present study that ionization rates measured in one spatial direction (e.g., for $0 < \theta < 15^\circ$) show also considerable sensitivity on the absolute phase, leading to a large, forward- to backward-signal ratio (along the polarization vector of a linearly polarized laser field) for certain laser phase values, which can be exploited in order to determine

experimentally the absolute phase and duration of a few-cycle laser pulse. In other words, we show that the absolute phase determines whether more electrons are emitted to one or the other side of an atom (along the laser polarization vector), as already suggested in [11]. Recently, the possibility of measuring this phase from angular distributions of photoelectrons, for circularly polarized laser pulses, was investigated both theoretically (using a quasistatic tunneling model) [9] and experimentally [11]. The theoretical analysis [9] based on a quasistatic tunneling model led to the conclusion that there exists a very simple relation between the electron angular distributions and the absolute carrier phase for circularly polarized light, whereas the absolute phase measurement using the linearly polarized light was predicted to be more difficult [9,11]. Our study indeed confirms that phase-dependent asymmetries depend on the intensity regime and on the pulse width, nevertheless we find the intensity regime in which the absolute phase effects yield a very clear signature in photoionization.

In this paper we report a detailed study of phase-induced spatial asymmetries for few-cycle, linearly polarized laser pulses interacting with a hydrogen atom. We solve numerically the three-dimensional TDSE for a hydrogen atom interacting with an intense few cycle laser pulse. We calculate the probability of detecting the photoelectron by measuring the electron signal in the forward ($\theta \approx 0^\circ$) and backward ($\theta \approx 180^\circ$) directions along the laser polarization. We find that the yield measured in a specific direction along the polarization vector varies significantly as a function of the absolute carrier phase. For example, at a laser intensity $I = 8 \times 10^{13} \text{ W/cm}^2$ ($\lambda = 800 \text{ nm}$) we observe that if detectors measure electrons in narrow polar angle intervals, e.g., $0^\circ - 15^\circ$, the signal can drop by a factor 2, reaching its maximum at the laser phase $\phi = \pi/4$ and its minimum at $\phi = 5\pi/4$. In other words, if the two detectors placed in opposite directions along the laser polarization vector measure the photoelectrons from a single shot, the forward-backward signal ratio can be equal to 2 for a few-cycle pulse, whereas it should be equal to 1 for long pulses. The above laser intensity, for which this ratio is so high, is slightly below the

Keldysh-tunneling regime [1]. We find that different, strong asymmetries also appear in the higher, barrier-suppression intensity regime. We believe that the above phase sensitivities of directional photoelectron emission can be used for experimental determination of the absolute carrier phase of a linearly polarized laser pulse.

More specifically, we solve the TDSE, using cylindrical coordinates and atomic units (i.e., $e = \hbar = m_e = 1$),

$$i \frac{\partial}{\partial t} \Psi(z, \rho, t) = - \frac{1}{2} \left(\frac{\partial}{\partial z^2} + \frac{\partial^2}{\partial \rho^2} + \frac{1}{\rho} \frac{\partial}{\partial \rho} \right) \Psi - (\rho^2 + z^2)^{-1/2} \Psi + z E(t) \Psi, \quad (1)$$

which describes the interaction of a hydrogen atom with a linearly polarized laser field $E(t)$ along the z axis. The numerical method we used was described earlier [12]. Our integration grid was defined by $|z| < z_{\max}$ and $0 < \rho < \rho_{\max}$, with $z_{\max} = 256$ bohr and $\rho_{\max} = 128$ bohr. We used the spatial steps $dz = d\rho = 0.25$ bohr and the integration step in time was 0.03 a.u. $= 7 \times 10^{-19}$ s. In order to avoid the reflections of the wave packet from the boundaries, the wave function was absorbed at $|z| > 240$ bohr and $\rho > 112$ bohr. We used the electric field $E(t)$ defined via the vector potential $A(t) = -c \varepsilon_0(t) \sin[\omega(t - t_M) + \phi] / \omega$,

$$E(t) = - \frac{1}{c} \frac{\partial}{\partial t} A(t) = \varepsilon_0(t) \cos[\omega(t - t_M) + \phi] + E_{\text{cor}}, \quad (2)$$

where $t_M = t_{\text{tot}}/2$, and

$$E_{\text{cor}} = \sin[\omega(t - t_M) + \phi] \frac{\partial}{\partial t} \varepsilon_0(t) / \omega$$

comes from the derivative of the envelope of the vector potential A . E_{cor} is small near the pulse maximum and is negligible for long pulses. We used the envelope $\varepsilon_0(t)$ in the following form:

$$\varepsilon_0(t) = E_0 \sin^2(\pi t / t_{\text{tot}}), \quad 0 < t < t_{\text{tot}}, \quad (3)$$

with $t_{\text{tot}} = 4$ cycles $= 10.6$ fs of the 800 nm, Ti:sapphire laser pulse. The pulses with an envelope described by Eq. (3) have a half-width of the intensity profile full width at half maximum $\tau_p = 2 \arccos(2^{1/4}) t_{\text{tot}} / \pi = 0.364 t_{\text{tot}}$, $\tau_p = 3.9$ fs for pulses shown in Fig. 1. For few-cycle pulses, we do not use $E(t)$ represented as an arbitrary electric field envelope times a trigonometric function since this may lead to a non-vanishing potential $A(t)$ at the end of the pulse [which is equal to the area under the $E(t)$ function]. By contrast, our definition, Eq. (2), of $E(t)$ via $A(t)$ (which has an arbitrary envelope) guarantees that $A(0) = A(t_{\text{tot}}) = E(0) = E(t_{\text{tot}}) = 0$. Figure 1 illustrates our definition of the absolute phase ϕ , Eq. (2): for $\phi = 0$, maxima of field and envelope coincide [Fig. 1(a)]; for $\phi = \pi/2$, the maximum of the envelope coincides with the zero of the field [Fig. 1(c)]; finally, for $\phi = \pi$, the maximum of the envelope occurs when the field reaches a minimum, Fig. 1(d). The numerical simulation was performed until the final time $t = t_f = 10$ cycles. Since we were interested in ionization signals measured in narrow angles in forward ($P_+, 0 < \theta < \theta_0$) and backward directions

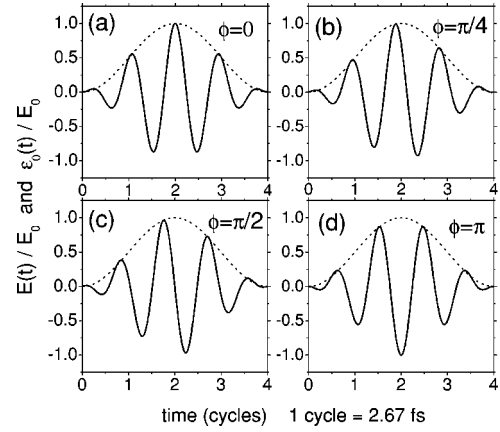


FIG. 1. Electric field $E(t)/E_0$ (solid) and its envelope $\varepsilon_0(t)/E_0$ (dotted) as a function of time in cycles for absolute phases: (a) $\phi = 0$; (b) $\phi = \pi/4$; (c) $\phi = \pi/2$; (d) $\phi = \pi$. The wavelength $\lambda = 800$ nm and the intensity profile half-width is $\tau_p = 3.9$ fs.

$P_-, 180 - \theta_0 < \theta < 180^\circ$ (we used $\theta_0 = 15^\circ$ or $\theta_0 = 30^\circ$), we performed the following integration of the probability flux near the absorbing boundaries during the simulation,

$$P_+ = 2\pi \int_0^{t_f} dt \int_0^{z_0 \tan(\theta_0)} d\rho \rho j_z(z_0, \rho, t),$$

$$P_- = -2\pi \int_0^{t_f} dt \int_0^{z_0 \tan(\theta_0)} d\rho \rho j_z(-z_0, \rho, t), \quad (4)$$

where

$$j_z(z, \rho, t) = \text{Re} \left[-i \Psi^*(z, \rho, t) \frac{\partial}{\partial z} \Psi(z, \rho, t) \right] \quad (5)$$

is the probability current along the z axis and we have chosen $z_0 = z_{\max}/2 = 128$ bohr. This choice ensures that the Coulomb force is negligible at such a large distance; in addition, we have $z_0 \gg E_0 / \omega^2$. The last condition ensures that a classical electron which reaches the distance $z = z_0$ after tunneling through the barrier will not return to the proton. We checked that z_0 is small enough to ensure that our “detector” placed at $z = z_0$ measures the total flux during our simulation time (larger z_0 would require larger simulation times). Thus P_+ and P_- are proportional to the yields of detectors placed at the right and left side of the atom along the z axis, which capture all electrons ionizing in directions $0 < \theta < \theta_0$ and $180^\circ - \theta_0 < \theta < 180^\circ$. For long pulses, because of inversion symmetry of the monochromatic electric field, yields of photoelectrons emitted in opposite directions are equal, i.e., $P_+/P_- = 1$. Thus we expect the ratio P_+/P_- [or $(P_+ - P_-)/(P_+ + P_-)$] to be an efficient measure of absolute phase effects, which break this forward-backward symmetry when ultrashort pulses are used. We show in Figs. 1(a) and 1(d) the most asymmetric electric field for $\phi = 0$ and $\phi = \pi$.

Because of the nonlinear character of atomic ionization in the long-wavelength regime, we expect strong directional effects for such an asymmetric field since the probability of tunneling (or via overbarrier ionization) just a half-cycle away from a maximum is considerably smaller than that at the envelope maximum. Indeed, Fig. 2(a) shows that in the

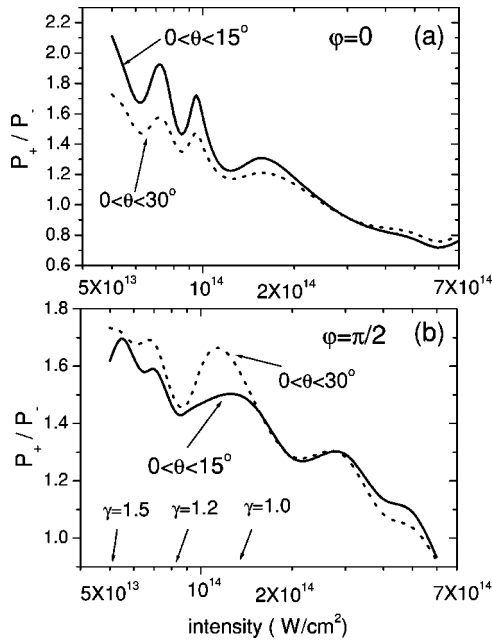


FIG. 2. Forward-backward probability ratios P_+/P_- as functions of the laser intensity I for (a) the absolute phase $\phi=0$, see $E(t)$ in Fig. 1(a), and for (b) $\phi=\pi/2$, see $E(t)$ in Fig. 1(c).

low-intensity regime ($I < 10^{14}$ W/cm²), the P_+/P_- ratio can even exceed 2, whereas at $I > 4 \times 10^{14}$ this asymmetry is reversed. This change is related to the fact that for $E_0 > I_p^2/4$ (or at $I > 1.4 \times 10^{14}$ W/cm²), where I_p is the atom's ionization potential ($I_p = 0.5$ hartree for hydrogen), the barrier is suppressed at the field maximum [8], whereas at lower intensity the tunneling mechanism predominates. Such a reversal of asymmetry has been previously noted in two-color ionization [6]. We display separately the probabilities P_+ , P_- as functions of phase ϕ in both regimes in Fig. 3: $I = 8.0 \times 10^{13}$ W/cm² (a) and $I = 6.0 \times 10^{14}$ W/cm² (b). These plots can be easily extended for phases $\phi > \pi/2$ with the help of the relations $P_+(\phi + \pi) = P_-(\phi)$ and $P_-(\phi + \pi) = P_+(\phi)$, which follow from the inversion symmetry of the atom and from the property $E(t, \phi + \pi) = -E(t, \phi)$. We note that for the laser intensity $I = 8.0 \times 10^{13}$ W/cm², P_+ has a broad maximum around $\phi = \pi/4$, with P_+/P_- considerably greater than 1 for ϕ ranging from 0 to $\pi/2$, whereas at higher intensities, Fig. 3(b), P_+/P_- is less than 1 for $\phi=0$ and close to 1 for $\phi=\pi/2$. The lower intensity [Fig. 3(a)] corresponds to the intermediate multiphoton-tunneling regime, since at $I = 8.0 \times 10^{13}$ W/cm² the Keldysh parameter $\gamma = \omega(2I_p)^{1/2}/E_0$ (where I_p is the atom's ionization potential) is equal to 1.19, i.e., one needs higher intensities, $I > 1.14 \times 10^{14}$ W/cm², in order to get to the tunneling regime. We interpret these asymmetries using the tunneling ionization model (with corrections resulting from Coulomb attraction of the electron, after tunneling [6]) at lower intensities, or the barrier suppression picture at higher intensities. In the latter case, Fig. 3(b), the observed asymmetry is very natural, since for $\phi=0$ the field is strongest in the positive direction of the z axis, [see Fig. 1(a)] and thus a negatively charged electron will preferen-

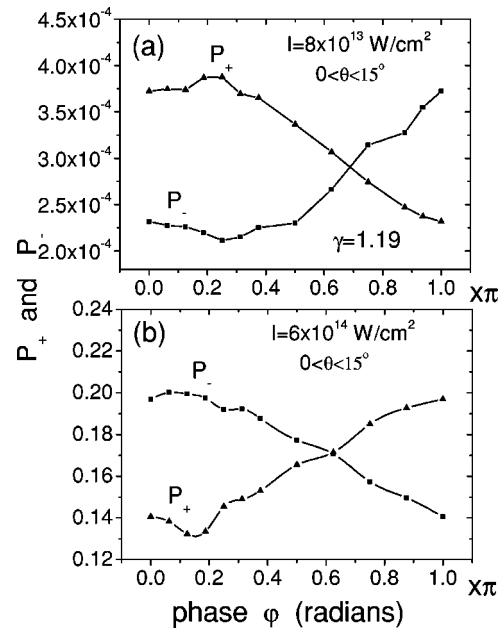


FIG. 3. Forward P_+ (Δ) and backward (\square) P_- probabilities as functions of the absolute phase ϕ for laser intensity (a) $I = 8 \times 10^{13}$ W/cm² and (b) $I = 6 \times 10^{14}$ W/cm².

tially go overbarrier backward (towards a negative z value) and will never return if its initial energy at the moment of leaving the barrier is sufficiently high. By contrast, for $\phi = \pi/2$ the electric field $E(t)$ is antisymmetric around the envelope peak and therefore symmetric overbarrier emission should occur, as seen in Fig. 2(b). For higher intensities, however, this symmetry will be lost since the probability of ionization during a half-cycle is close to 1, causing considerable depletion of the initial-state population during the half-cycle at which the field is negative. Similarly, intuitive asymmetry in the overbarrier regime for $\phi=0$ will be altered at $I > 6 \times 10^{14}$ W/cm² because of the depleted initial-state population during the rise of the pulse.

In the lower-intensity range, $I < 2 \times 10^{14}$ W/cm², the electron ionizes via tunneling, leading to counterintuitive asymmetries similar to those occurring for two-color laser pulses discussed by us earlier [6]. We explain these asymmetries using a two-step ionization model [4,6], in which the electron first tunnels instantaneously at $t=t_0$ through the barrier and, in the second step, moves as a classical particle driven by the force $-E(t) - \partial V_C/\partial z$ [where $V_C(z, \rho)$ is the Coulomb potential], with the initial velocity $v(t_0) = 0$. As in [6], for $\phi = \pi/2$ we obtain more forward (P_+) electrons by neglecting the Coulomb potential V_C in the Newton equation of motion and solving it analytically. We thus get

$$z(t) = z(t_0) + \frac{1}{c} \int_{t_0}^t A(t') dt' + (t - t_0) v_d, \quad (6)$$

$$v_d = -\frac{1}{c} A(t_0) = \frac{\varepsilon(t_0)}{\omega} \sin[\omega(t_0 - t_M) + \phi],$$

where $z(t_0)$ is the point at which the electron leaves the barrier. This results means that the sign of v_d determines the

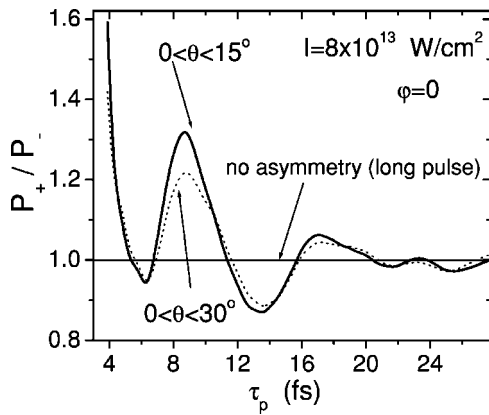


FIG. 4. Forward-backward probability ratios P_+/P_- as functions of the pulse duration τ_p at laser intensity $I=8 \times 10^{13}$ W/cm², for $\phi=0$.

asymmetry. For $\phi = \pi/2$, Fig. 1(c), we checked that at the maximum and at the minimum of $E(t)$ (i.e., when the tunneling probability is maximum), the drift velocity is positive, $v_d = 0.08$ a.u., therefore we expect from this simple model more electrons forward ($z > 0$), as seen in Fig. 3(a) or in Fig. 2(b). For $\phi = 0$, however, this simple model predicts symmetric photoemission, since $v_d = 0$ at the peak of the field $E(t_0)$, the tunneling probability is symmetric around the peak, and v_d is antisymmetric. This agrees with the results of our simulations at $I = 2.5 \times 10^{14}$ W/cm², however it disagrees with asymmetries occurring at lower intensities. We believe that the preponderance of forward electrons at lower intensities for $\phi = 0$ originates from the Coulomb attraction neglected when solving the Newton equation of motion, which causes the electron to go in the counterintuitive direction, $z > 0$, for the case in which tunneling occurs at $z(t_0) < 0$. For the case of a two-color laser [6] (for the relative phase $\phi = 0$), the electric field is in fact similar to that in Fig. 1(a), and we have demonstrated in [6] by solving the complete Newton equation that inclusion of the Coulomb attraction in the electron dynamics after tunneling explains quantitatively the asymmetries seen in the exact quantum calculations. Summarizing, our results are in agreement with the predictions of a simple tunneling model for $\phi = 0$ and $\phi = \pi/2$, at intensity around 2×10^{14} , and are “intuitive” in

the barrier-suppression regime. Finally, let us note that the pulse duration $\tau_p = 3.9$ fs, chosen in our paper, is slightly shorter than that currently used in experiments [1]; however, going below $\tau_p = 4.5$ fs seems feasible [13]. Therefore, we performed a series of simulations for longer pulses and we display the results in Fig. 4. We note that the asymmetry falls off rapidly as a function of pulse duration. For $\tau_p = 4.5$ fs, $P_+/P_- = 1.17$ at $I = 8 \times 10^{13}$ W/cm² and it becomes much larger at lower intensity, $I = 5 \times 10^{13}$ W/cm², when $P_+/P_- = 1.53$ for $\tau_p = 4.6$ fs and $\phi = 0$. Clearly, these numbers suggest that measurement of the asymmetry P_+/P_- ratio in the subtunneling regime (i.e., for $\gamma > 1.1$), accompanied with numerical simulations, can be useful for the determination of the pulse duration and its absolute phase, e.g., our results suggests that just detecting large asymmetries ($P_+/P_- > 1.5$) would be a clear signature that the pulse duration is shorter than 1.5 cycles. Note that asymmetries do not fall off monotonically as a function of the pulse width τ_p . The reason for this is probably the following: for the shortest pulse, the envelope falls off so rapidly that only tunneling from the pulse maximum contributes, whereas for $\tau_p = 5$ fs the tunneling from the two lowest pulse minima contributes, and so on for longer pulses, leading to the oscillations in Fig. 4. Furthermore, our numerical simulations show the importance of including the Coulomb potential in tunneling models, as previously discussed in relation to two-color ionization [6]. Its inclusion leads to Coulomb focusing, clearly seen in Fig. 2(a), where at low intensities the asymmetry is much larger when measurement is done in a very narrow angle interval ($0 < \theta < 15^\circ$, solid line) than in a broader interval (dotted line). The opposite happens in Fig. 2(b), $\phi = \pi/2$ (i.e., dotted line is higher than the solid), where Coulomb focusing is the same in both the forward and backward directions. The oscillations seen in Fig. 2 are also, probably related to the wave packet which was highlighted by Coulomb forces and which interferes with a directly ionizing wave packet. Clearly, more detailed studies of angular distributions are necessary to explain completely the above peculiarities.

We thank the Natural Sciences and Engineering Research Council of Canada for the financial support, and Dr. P. H. Bucksbaum, Dr. P. B. Corkum, and Dr. H. S. Nguyen for helpful discussions.

- [1] T. Brabec and F. Krausz, *Rev. Mod. Phys.* **72**, 545 (2000); Q. Apolonski *et al.*, *Phys. Rev. Lett.* **85**, 740 (2000); C. Spielman *et al.*, *Science* **278**, 661 (1997).
 [2] K. J. Schafer and K. C. Kulander, *Phys. Rev. A* **45**, 8026 (1992).
 [3] Zhen-Min Wang and D. S. Elliott, *Phys. Rev. Lett.* **87**, 173001 (2001), and references therein.
 [4] D. W. Schumacher and P. H. Bucksbaum, *Phys. Rev. A* **54**, 4271 (1996).
 [5] B. Sheehy, B. Walker, and L. F. DiMauro, *Phys. Rev. Lett.* **74**, 4799 (1995).
 [6] S. Chelkowski, M. Zamojski, and A. D. Bandrauk, *Phys. Rev.*

- A* **63**, 023409 (2001); A. D. Bandrauk and S. Chelkowski, *Phys. Rev. Lett.* **84**, 3562 (2000).
 [7] T. Zuo and A. D. Bandrauk, *Phys. Rev. A* **54**, 3254 (1996).
 [8] I. P. Christov, *Appl. Phys. B: Lasers Opt.* **70**, 459 (2000); *Opt. Lett.* **24**, 1425 (1999).
 [9] P. Dietrich, F. Krausz, and P. B. Corkum, *Opt. Lett.* **25**, 16 (2000).
 [10] A. de Bohan *et al.*, *Phys. Rev. Lett.* **81**, 1837 (1998).
 [11] G. G. Paulus *et al.*, *Nature (London)* **414**, 182 (2001).
 [12] T. Zuo *et al.*, *Phys. Rev. A* **51**, 3991 (1995).
 [13] P. B. Corkum (private communication).